J Mol Model (2011) 17:477–493
DOI 10.1007/s00894-010-0745-1

ORIGINAL PAPER

Insights into subtype selectivity of opioid agonists by ligand-based and structure-based methods

Jianxin Cheng · Guixia Liu · Jing Zhang · Zhejun Xu · Yun Tang

Received: 20 February 2010 / Accepted: 4 May 2010 / Published online: 25 May 2010

Abstract To probe the selective mechanism of agonists binding to three opioid receptor subtypes, ligand-based and receptor-based methods were implemented together and subtype characteristics of opioid agonists were clearly described. Three pharmacophore models of opioid agonists were generated by the Catalyst/HypoGen program. The best pharmacophore models for μ, δ and κ agonists contained four, five and five features, respectively. Meanwhile, the three-dimensional structures of three receptor subtypes were modeled on the basis of the crystal structure of β2-adrenergic receptor, and molecular docking was conducted further. According to these pharmacophore models and docking results, the similarities and differences among agonists of three subtypes were identified. μ or δ agonists, for example, could form one hydrogen bond separately with Tyr129 and Tyr150 at TMIII, whereas κ ones formed a π-π interaction in that place. These findings may be crucial for the development of novel selective analgesic drugs.

Keywords Homology modeling · Molecular docking · Opioid receptors · Opioid receptor agonists · Pharmacophore · Receptor-ligand interaction

Electronic supplementary material The online version of this article (doi:10.1007/s00894-010-0745-1) contains supplementary material, which is available to authorized users.

J. Cheng · G. Liu (✉) · J. Zhang · Z. Xu · Y. Tang (✉)
Laboratory of Molecular Modeling & Design, School of Pharmacy, East China University of Science and Technology, 130 Meilong Road,
Shanghai 200237, China
e-mail: gxliu@ecust.edu.cn
e-mail: ytang234@ecust.edu.cn

Introduction

For centuries, in treatment of severe pain, no new analgesics can replace opium and its derivatives. Morphine isolated from opium is one of the most widely used opioid analgesics today. Many efforts have been focused on opioid pharmacology [1–4]. Currently, potent analgesics, such as morphine and fentanyl, are popular, but the pharmacology evidence has already indicated that the addiction effect of these analgesics is mainly attributed to activating μ opioid receptor. So, understanding the mode of μ subtype-agonist interaction will be necessary for clarifying the addictive mechanism. The δ subtype is an essential partner for opioid action. δ opioid receptor has the ability to modulate the unwanted effects of μ subtype agonists and δ opioid receptor plays an important role for pain action[5–7]. Many experiments have proved that a few κ agonists are also able to produce strong analgesic effect but without addiction [8–10]. Therefore, developing specific κ opioid receptor agonists is also an interesting topic.

The rational design of drugs for a specific target is greatly aided by structural information of the target. The G-protein coupled opioid receptor is not an exception. However, there is no experimental structure available for developing drugs for these receptors. In the absence of an experimentally obtained crystal structure of these targets, researchers displayed their excellent genius. Many different but reliable methods were developed and applied, such as 3D-QSAR, pharmacophore modeling and homology modeling. Choosing suitable methods for different situations, will yield meaningful results.

In the 1970s, QSAR method was used for developing new opioid agonists [11, 12]. With the development of computational chemistry, 3D-QSAR was also used for exploring the structure-activity relationship for almost all

kinds of opioid agonists [13–17]. Recently, many new agonists interacting with opioid receptors were reported with greater diversity in both chemical structures and biological activity [10, 18–50]. Therefore, new information about structure-activity relationship based on numbers of these compounds with greater diversity should be helpful for 3D-pharmacophore modeling. From these reliable pharmacophore models, we can not only separately get respective chemical features for agonists of μ, δ and κ subtype, but also carry on virtually screening to obtain new leads for certain subtype.

For many years, rhodopsin had been an only G protein-coupled receptor (GPCR) with available crystallographic structural information [51–53]. Based on rhodopsin, opioid receptors were modeled and used for docking or simulation [54–58]. In November 2007, a new high-resolution crystal structure of GPCR, β_2 adrenergic receptor (β_2-AR), was reported. This was a greatly important progress for drug research of GPCR [59, 60]. Because of its higher sequence identification than rhodopsin, it's a new chance to understand the mode of interaction for opioid receptors and their agonists.

In this study, a ligand-based method, pharmacophore modeling was applied to extract common and specific chemical features for three opioid receptor subtypes. Then, homology models of μ, δ and κ opioid receptors were constructed based on the crystal structure of β_2-AR. And interactions between each opioid receptor and their specific agonists were explored by subsequent molecular docking. At last, docking complexes together with pharmacophore models were built, with aims to understand the detailed interactive mode of every subtype-agonist interaction. From the series of ligand-based or structure-based molecular modeling, characteristics of each subtype-agonist interaction were clearly described. The specific information for every subtype would be a useful reference for designing new analgesics.

Materials and methods

Pharmacophore modeling

Training set selection In order to fulfill the need that the diversity of compounds is as large as possible both in scaffold and in activity, tens of references were retrieved. From these references, 103 specific μ opioid agonists, 130 δ opioid agonists and 92 κ opioid agonists had been collected. The configuration of all these compounds was clear. Considering significant structural diversity and wide coverage of molecular bioactivities, we selected 20, 22 and 21 compounds as training set for μ, δ and κ subtype, separately. In these training sets, many classic agonists were included, such as morphine analogues(Cm2) [18], SNC80 analogues(Cd1) [19] and ICI199441(Ck1) [20] (Table 1). To validate our pharmacophore hypothesis, the rest collected compounds with available K_i values were used as test set.

All 2D chemical structures were produced with the ISIS/Draw version 2.5 drawing program, and the conformational analysis for each molecule was implemented using the Poling algorithm [61] and CHARMM force field parameters [62] within the Catalyst software package. Poling is a method for prompting conformational variation that forces similar conformations away from each other. A maximum number of 250 conformations of each compound were selected using "best conformer generation" option with a constraint of 20 kcal mol^{-1} energy thresholds above the minimum conformer searched to ensure an exhaustive characterization of conformational space. All other parameters were kept at their default settings.

Pharmacophore model generation Based on the conformations for each compound, Catalyst/HypoGen mode was employed to construct possible pharmacophore models [63]. Analysis of functional groups on each compound in training set revealed that four chemical features, hydrogen-bond acceptor (HBA), hydrophobic group (HY), positive ionizable point (PI) and ring aromatic group (RA), could effectively map nearly all of the critical chemical groups. Hence, these four features were selected to form the essential information in this hypothesis generation process. The count of these features was set from 0 to 5, except PI from 1 to 5, because PI was an essential feature for opioid receptor agonists.

The pharmacophore model produced by HypoGen identifies chemical functional features that are typical of active compounds, thus facilitating their differentiation from inactive compounds. When generating a hypothesis, Catalyst/HypoGen attempts to optimize the pharmacophore models based on the experimental values and the complexity of the hypothesis. The default uncertainty value of three was used for the compound activity, representing the ratio of the uncertainty range of measured biological activity against the actual activity for each compound [64]. To further test the predictability of these pharmacophore models, r_m^2 is calculated as $r_m^2 = r^2*(1 - \mathrm{sqrt}(r^2 - r_0^2))$ based on the test set according to Roy and Roy [65].

Homology modeling

On the basis of new β2-AR crystal structure, reliable homology models of human opioid receptors were built by program Modeler [66, 67]. In all cases, the one disulfide bridges in the EL2 were manually defined. For every alignment, three models were built, and each of them was

subjected to five loop refinements setting the optimization level to high. The quality of these models was examined in terms of residue-based probability density function and residue-based energy, as calculated by Modeler. For every one of the alignments, the soundest models were chosen for the subsequent docking experiments.

Molecular docking

Protein and ligand preparation Ligands, such as Cm2, Cd1 and Ck1, were sketched in Maestro and subjected to a Monte Carlo multiple minimum conformational search using the OPLS_2005 force field and water as implicit solvent (surface generalized Born (SGB) model) [68, 69]. The lowest energy conformation of the ligand was used as the starting point for the docking experiments.

Opioid receptor models were imported into the Maestro interface of the Schrödinger software and subjected to the protein preparation workflow to (1) add hydrogens; (2) detect the disulfide bonds; (3) optimize the H-bond alignment; and (4) perform a constrained refinement by hydrogens only option with the *impref* utility. The *impref* utility consists of a cycle of energy minimization based on the *impact* molecular mechanics engine and on the OPLS_2001 force field utility, setting the max RMSD of 0.30. If, at the end of any minimization cycle, the RMSD of the heavy atoms is greater than the max RMSD from the original structure, the calculation terminates and returns the structure resulting from the previous cycle. Here, it's unnecessary to optimize the heavy atoms, so hydrogens only option was selected and heavy atoms were left in place.

Induced fit docking Molecular docking was performed with the induced fit docking procedure based on Glide 5.0 and Prime 2.0, as implemented in the Schrödinger package [70, 71]. The procedure is composed by a Glide SP docking, followed by a Prime refinement of side chains of the residues in the binding pocket and then by a final Glide XP docking of the ligand into the receptor in the refined conformations.

The docking box of every model was centered on Tyr150 of μ receptor, Tyr129 of δ receptor and Tyr 139 of κ receptor, and was featured a side of 26 Å. In the initial Glide SP docking (Glide 5.0), the vdW scaling was set to 0.5 for nonpolar atoms of receptor and ligand. For each obtained docking pose, a Prime refinement (Prime 2.0) was performed on all the residues located within 5 Å from the ligand. Briefly, the Prime refinement starts with the optimization of the side chains of the selected residues performed through randomization and subsequent exploration of various combinations of rotamers; the optimization is followed by a truncated-NeSwton minimization of the selected residues and the ligand using the OPLS_2000 all-atom force field for the receptor and OPLS_2001 for the ligand, treating solvation with the SGB continuum solvation model. All the obtained complexes within an energy range of 30 kcal mol^{-1} from the best were passed on to the final step, in which the ligand was extracted and redocked with Glide XP (Glide 5.0), with a vdW scaling factor of 0.8 for the non polar atoms of the ligand only.

Mapping above pharmacophore models onto their corresponding docking complexes

After generating pharmacophore models and docking complexes, the best pharmacophore models were superimposed into the active sites of their corresponding docking complexes by the protocol implemented in Discovery Studio 2.1. The pharmacophore features and key residues were further carefully analyzed.

Results

Pharmacophore modeling

Biological activity data and training set selection

From all available references, we collected all kinds of agonists with available K_i for every opioid receptor subtype. From these references, 103 specific μ opioid agonists, 130 δ opioid agonists and 92 κ opioid agonists have been collected [10, 18–50]. The structure of all these compounds was clear.

The compounds were divided into two sets: training set and test set. The selection of a suitable training set is critical for the quality of automatically generated pharmacophore models. We selected training set with following two rules [72]: (a) both training and test sets should have structures from each class of compounds to ensure structural diversity. If one class has only one compound, it was assigned to training set; (b) both training and test sets should cover molecular bioactivities (K_i) as wide as possible. If there is only one compound with maximum or minimum order of bioactivity in a class, this compound was assigned to training set.

To ensure the statistical relevance of generated models, training set should contain a set of diverse compounds together with their activity values. These should originate from comparable binding assays and spread equally over at least 4–5 orders of magnitude. Ligand binding assays were determined for compounds at μ, δ and κ opioid receptors as described in detail in many reports [73, 74]. Binding affinities for μ, δ and κ receptors were determined by displacing, respectively, ^{3}H-DAMGO, ^{3}H-DPDPE and ^{3}H-diprenorphine from membranes prepared from cells

expressing cloned human opioid receptors. Subtype selectivity over other opioid receptors was defined by the ratio of the K_i values. Each selected compound should be contributed to its corresponding model, both in terms of structural features and activity range, yet avoiding redundancy and bias. The most active compounds should be included because they could illustrate critical information on pharmacophore requirements.

On the basis of above criteria, representative compounds were selected as training set (Table 1). As pharmacophore models were semi-quantitative classification models and for the purpose of estimation (prediction), all compounds were classified by their activity as highly active (K_i<10 nM, +++), moderately active (10 nM≤K_i≤500 nM, ++) or inactive (K_i>500 nM, +).

Generation of pharmacophore hypotheses

In order to generate a reasonable pharmacophore hypothesis, some parameters must be cared for, such as cost value, fitness, mapped features, relevance and so on. Among them, cost analysis was the most important for the quality of a pharmacophore model.

In addition to generating hypotheses, Catalyst 4.10 also performed two important theoretical cost calculations (represented in bit units) directly determining whether any of pharmacophore hypothesizes was successful. First, Fixed cost was the cost of an ideal hypothesis, which represented the simplest model that fitted all data perfectly. Second, Null cost was the cost of the null hypothesis, which represents the highest cost of a pharmacophore without feature and whose estimated activity was the average of the activity data of the training set molecules. They represented the upper and lower bounds for generated hypotheses. According to randomized studies, a cost difference of 40–60 between its Total cost and its Null cost indicates a 75–90% chance of representing a true correlation in the data.

In Table 2, a set of the best pharmacophore hypotheses was showed. For every subtype, a set of 10 pharmacophore hypotheses was generated from corresponding training set. Parameters of these hypotheses, which included different cost values calculated during hypotheses generation along with RMS, Correlation(r) and pharmacophore features. From Table 2, we could clearly find that, for good hypotheses, the value of Total cost of each hypothesis was close to Fixed cost value against Null cost. In this study, for μ subtype, the Total cost of the best hypothesis was 102.56 and Fixed cost of the run was 80.68. The cost of null hypothesis for all 10 hypotheses was 168.28. The difference between Null cost and Total cost was 65.72 bits, which was over the 60 bits range, so it showed that the top-ranked hypothesis, Hypo1, had over 90% probability of correlating the data. For δ and κ subtypes, the differences between Null cost and Total cost was 89.76 and 61.24 bits, separately, which was over the 60 bits range, so it showed that the top-ranked hypothesis for δ or κ, Hypo1, also had over 90% probability of correlating the data.

Hypo1 showed the best values in all kinds of parameters, such as the highest ΔCost, error value, the lowest RMS deviation, and the highest correlation coefficient (Table 2). Therefore, Hypo1 was selected as the best pharmacophore. For μ subtype, the best model consisted of four features: two hydrogen-bond acceptor (HBA), one ring aromatic (RA) and one positive ionizable function (PI) (Fig. 1a). For δ subtype, the best model consisted of five features: one HBA, three hydrophobic points (HY) and one PI (Fig. 1b). For κ subtype, the best model consisted of five features: one HBA, two HY, one RA and one PI (Fig. 1c). The models above also showed spatial arrangement of chemical features in Fig. 1, and the actual and estimated K_i values of training set compounds were shown in Table 3.

For the training set in every Hypo1, the most active molecules were predicted as active (+++), one moderately active compound, Ck14, was predicted as inactive (+) and two inactive compounds, Cm19 and Cd19, were predicted as moderately active (++). For the three compounds, the difference between their actual and estimated activity observed was about 1 order of magnitude, which might be an artifact of the program that uses a different number of degrees of freedom for these compounds to mismatch the algorithm.

The error factor is also reported in Table 3. It shows that all the molecules in the training set have errors less than 20, except Ck14, which means that the activity prediction of these compounds falls between 20-fold greater and 1/20 of the actual activity. More exciting, most of the molecules have errors less than 10, which indicates that the activity prediction of these compounds falls between 10-fold greater and 1/10 of the actual activity.

Validation of pharmacophore models

Mapping Hypo1 to compounds with highest estimated values For these active compounds (+++), they should be completely mapped to respective Hypo1. From Fig. 2, we could see that all highly active compounds were completely mapped to Hypo1, separately, and the final conformations were stretched. Besides, each subtype showed its separate mapping characteristics from mapping. For example, for μ subtype, nearly all the compounds in the training set mapped the two HBA features, which revealed that this feature could be largely responsible for the high μ subtype molecular bioactivity.

Activity prediction To validate our pharmacophore, the other available compounds that are not in the training

Table 1 Training set of (A) μ, (B) δ and (C) κ agonists. All 2D structures were drawn with program ISIS/Draw, version 2.5

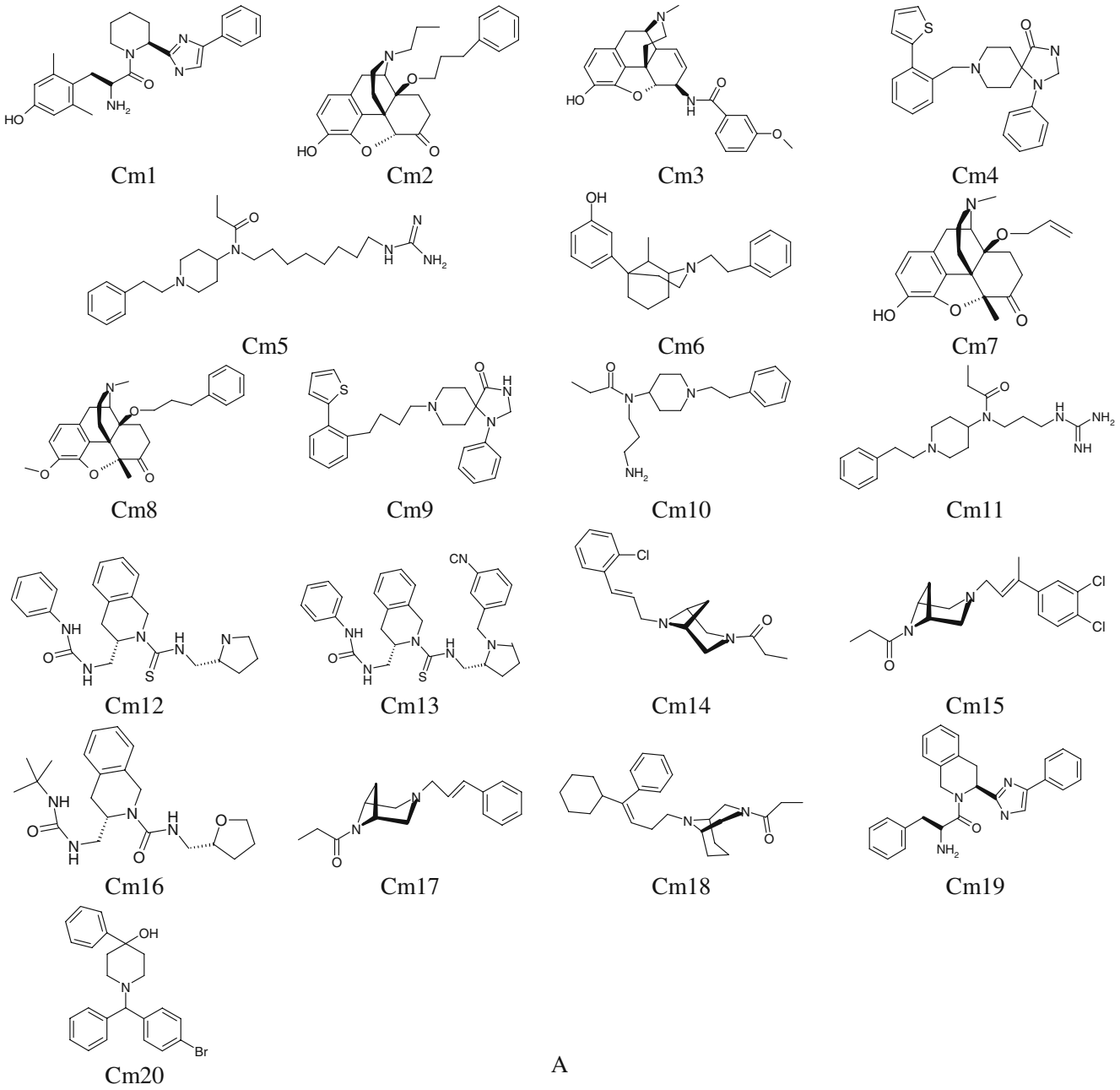

set were used as the test set. Through the simple validation, we got rational results. For the best hypothesis, the correlation of test set was 0.760, 0.730, and 0.734 for μ, δ and κ subtype, separately (Fig. 3). Besides, compounds distributed uniformly in accord with respective structure type. In summary, most of the compounds in test set were predicted correctly for their biological activity.

Besides r, we also calculated the r^2 and r_m^2 values for the test set [64]. As shown in Table 4, for all the three subtypes, the r^2 values were more than 0.5, while the r_m^2 values were less than 0.5, especially for κ subtype.

Homology modeling and molecular docking

After the crystal structure of β2-AR was determined in 2007 [59], it's very interesting to model opioid receptors based on the high-resolution crystal structure. From Daniel's analysis [60], AR-T4L retained high binding affinity for agonists, and so adrenergic receptor was an excellent

Table 1 (continued)

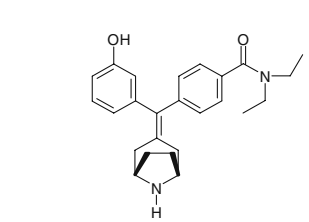

Cd1

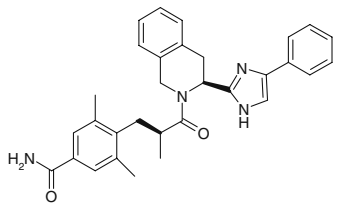

Cd2

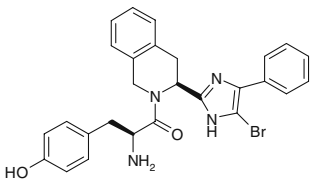

Cd3

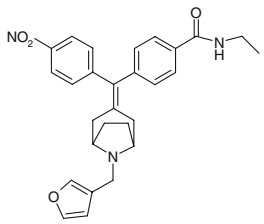

Cd4

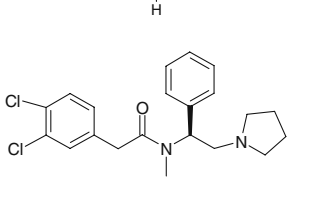

Cd5

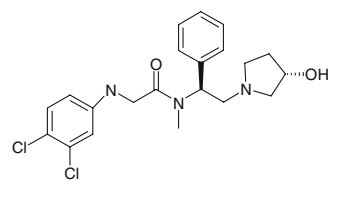

Cd6

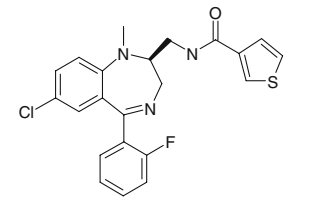

Cd7

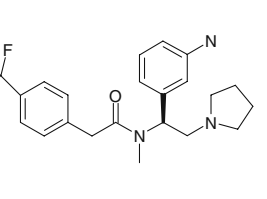

Cd8

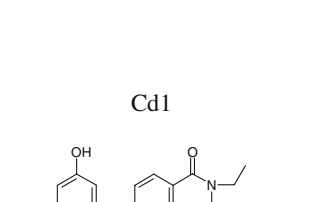

Cd9

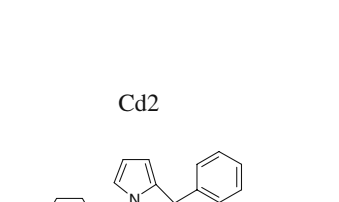

Cd10

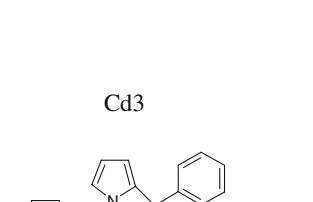

Cd11

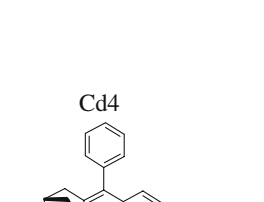

Cd12

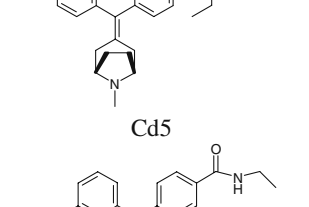

Cd13

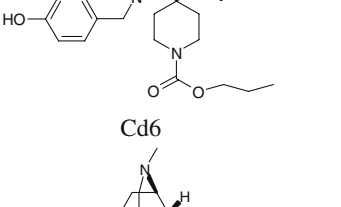

Cd14

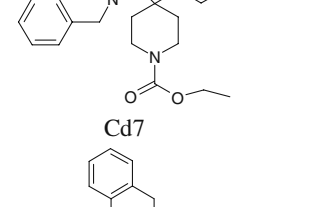

Cd15

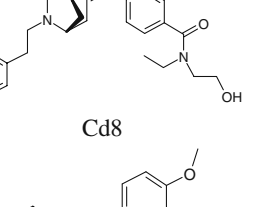

Cd16

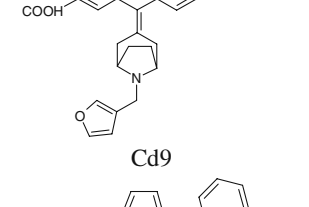

Cd17

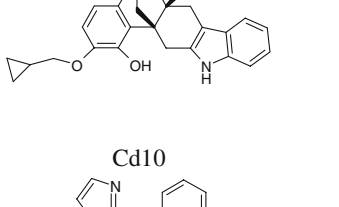

Cd18

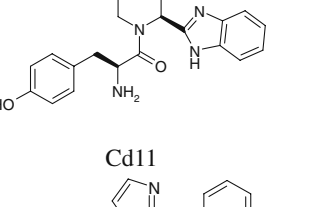

Cd19

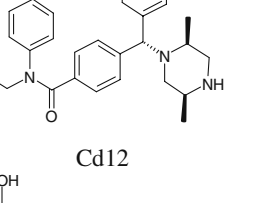

Cd20

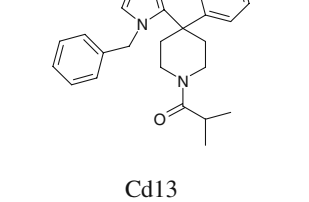

Cd21

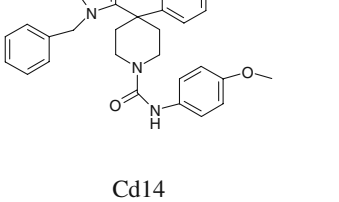

Cd22

B

Table 1 (continued)

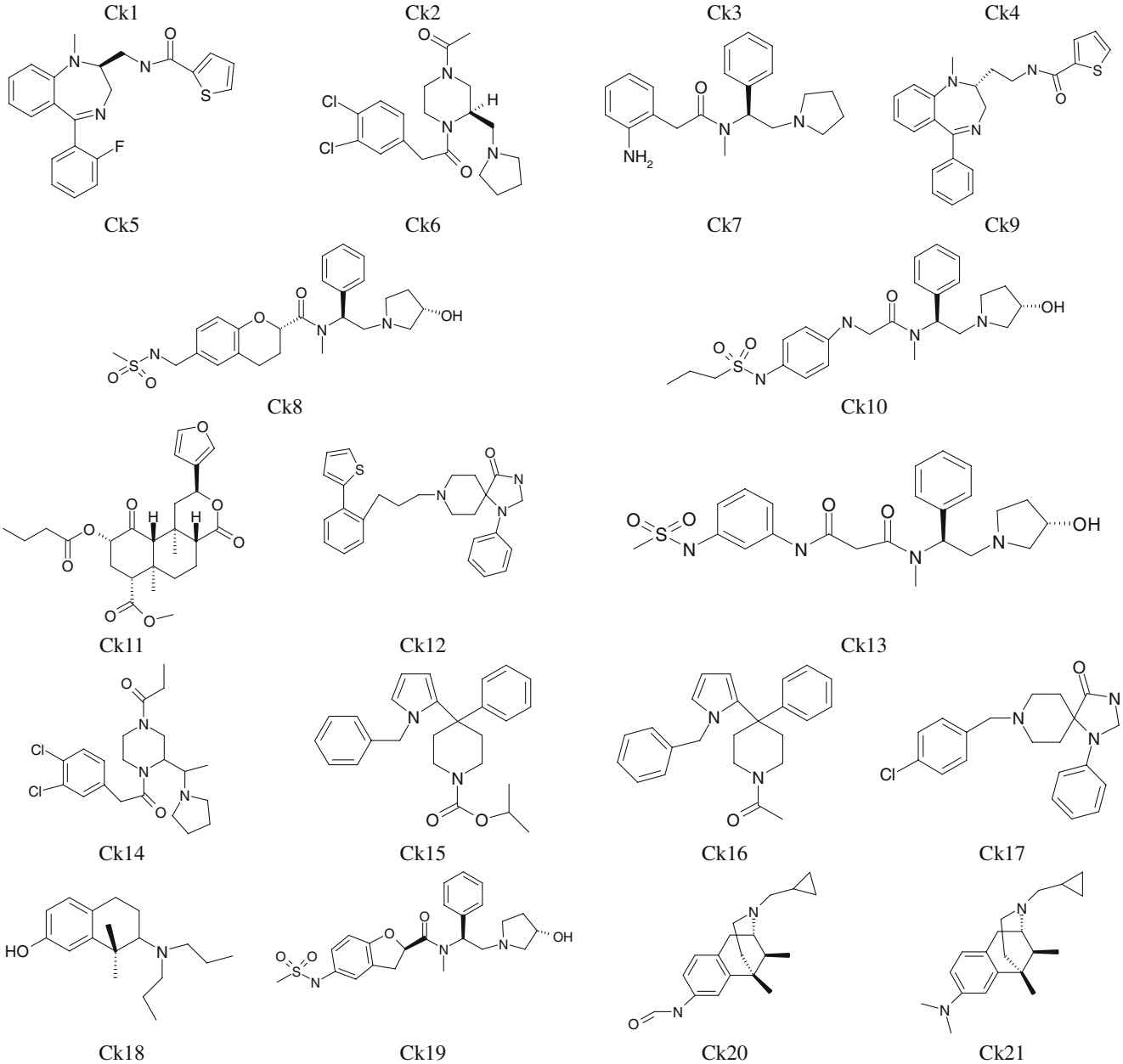

C

template for modeling the active receptor before new crystal structure complexed with agonists was obtained.

3D structures of three opioid receptor subtypes were modeled by homology modeling (Fig. 4). The RMSD value of the best models with the template 2RH1 was 1.69, 1.77 and 1.82 respectively for μ, δ and κ subtype. These models were examined by PROCHECK program. The results from PROCHECK were very satisfactory: 98% of these residues of every subtype were placed in the allowed area, and none of the remains placing in the unallowed area were key residues. Therefore, these models were reliable and feasible.

After above homology models were constructed, representative ligands, such as morphine analogue, SNC80 analogue and ICI199441, were selected and docked into them by means of induced fit procedure implemented in Schrödinger package. For these molecules, the estimated values were highest. The procedure was used for exploring the flexibility of both ligands and receptors in the course of docking process.

Table 2 Results of top 10 pharmacophore hypotheses generated from each training set[a] using program Catalyst/HypoGen

μ opioid agonists hypothesis					δ opioid agonists hypothesis				κ opioid agonists hypothesis				
No.	Features[b]	Total cost	Δcost	Cor.(r)	No.	Features	Total cost	Δcost	Cor.(r)	No.	Features	Total cost	Δcost	Cor.(r)
Hm[c]1	AAPR	102.56	65.72	0.948	Hd[c]1	AHHHP	112.79	89.76	0.930	Hk[c]1	AHHPR	102.41	61.24	0.910
Hm2	AAPR	105.23	63.05	0.909	Hd2	AHHHP	114.58	87.97	0.923	Hk2	AHHPR	107.08	56.57	0.877
Hm3	AAPR	105.97	62.31	0.910	Hd3	AHHHP	120.40	82.15	0.884	Hk3	AHPR	111.35	52.33	0.863
Hm4	AAPR	107.01	61.27	0.906	Hd4	AHHHP	129.51	73.04	0.850	Hk4	AHPR	112.57	51.08	0.853
Hm5	AAPR	111.40	56.88	0.847	Hd5	AHHHP	137.25	65.30	0.805	Hk5	AHPR	113.85	49.80	0.835
Hm6	AAPR	111.72	56.56	0.856	Hd6	AHHHP	142.27	60.28	0.752	Hk6	AHHPR	114.21	49.44	0.832
Hm7	AAPR	113.52	54.76	0.830	Hd7	AHHHP	153.85	48.70	0.689	Hk7	AHHPR	114.67	48.98	0.828
Hm8	AAHP	113.78	54.50	0.829	Hd8	AHHPR	157.94	44.61	0.666	Hk8	AHPR	115.03	48.62	0.834
Hm9	AAPR	113.81	54.47	0.826	Hd9	AHHPR	158.78	43.77	0.661	Hk9	AHPR	115.07	48.58	0.825
Hm10	AAPR	114.94	53.34	0.817	Hd10	AHHPR	158.82	43.73	0.661	Hk10	AHPR	115.32	48.33	0.845

[a] For μ subtype, Null cost = 168.28; Fixed cost = 80.68; Configuration cost =12.28; For δ subtype, Null cost = 202.55; Fixed cost = 86.37; Configuration cost =11.25; Forκsubtype, Null cost = 163.65; Fixed cost = 85.41; Configuration cost =13.65. All cost units are in bits. Configuration cost: a Fixed cost which depends on the complexity of the hypothesis space being optimized

[b] A, hydrogen-bond acceptor; H, hydrophobic feature; P, positive ionizable feature; R, aromatic ring feature

[c] Hm is the shortcut of the hypothesis of mu subtype, Hd is that of delta and Hk is that of kappa

The docking procedure yielded many similar poses. From them, best results which had a higher score, a more clear interaction, and a more rational side-chain orientation were finally selected (Fig. 5). Hydrogen bond interaction is a most important interaction, and so this interaction should be clear in the docking results. Side-chain orientation, especially the aromatic ring, is a critical aspect for correct poses. These side-chains should not appear clear errors, such as cross or overlapping and so on. Based on these best complexes, we could clearly see those key residues which joined receptor-agonist interaction, and those ones that were related to the interaction.

Pharmacophore mapping with their corresponding docking complexes

After docking analysis, ligand poses were extracted and mapped to corresponding pharmacophore models by Discovery Studio 2.1. These results (Fig. 6) obtained by ligand-based and structure-based methods could more clearly described mode of receptor-ligand interaction than those only shown by pharmacophore mapping (Fig. 2), and more clearly than those only shown by docking analysis.

Discussion

Pharmcophore modeling

Insights into chemical features from Hypo1 of every type

Based on Table 3, we calculated the sensitivity (SE), which is defined as (true positives)/(true positives + false negatives) and specificity (SP), which is defined as (true negatives)/(true negatives + false positives) for the best models. From Table 4, we could see that SE value for every subtype was much larger than its respective SP value. Therefore, we could say that the best models were very sensitive to active compounds. According to new r_m^2 method, we also calculated the r^2 and r_m^2 values in Table 4 [65]. For all three subtypes, the r^2 values were more than 0.5, and therefore our pharmacophore models were acceptable. However, in accord with Ref. [65], simple r^2 is not a good indicator of predictability of models, and then it's necessary to provide r_m^2 values. Table 4 shows all the r_m^2 values of models for three subtypes were less than 0.5. r_m^2 values were not acceptable reflecting considerable differences in r^2 and r_0^2 values, especially for κ subtype. And this indicates the predictability of the models may not be very high. This may be caused by great diversity in molecular structure type and biological activity.

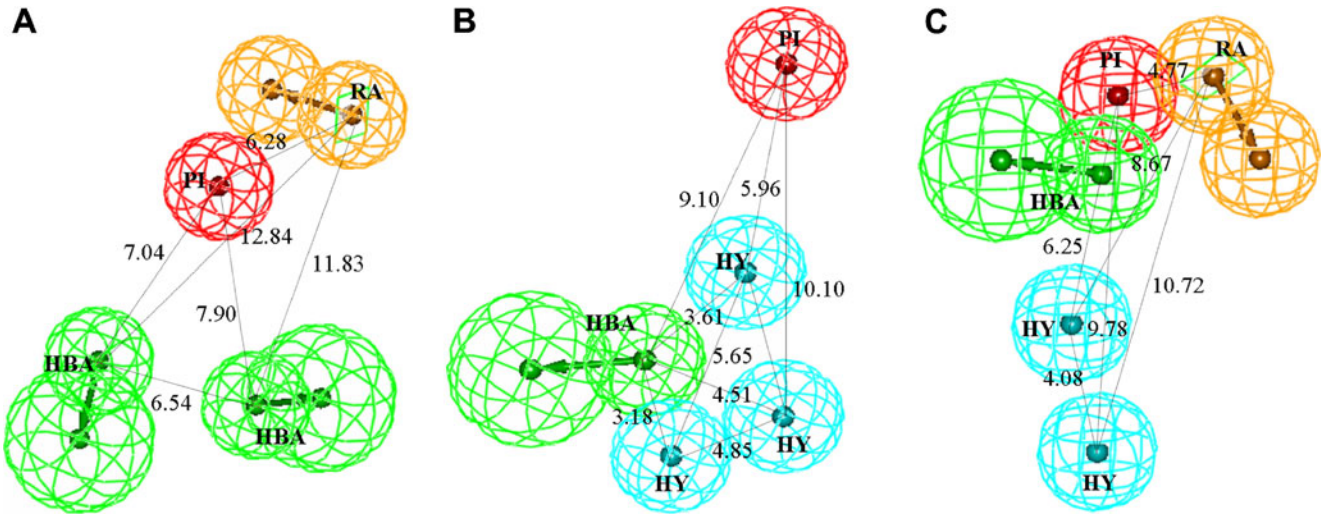

Fig. 1 The best hypothesis models produced by the HypoGen module in Catalyst4.10 software package. (**a**), (**b**) and (**c**) were the agonist-pharmacophore models of μ δ and κ subtype, separately. Pharmacophore features are color-coded with light-blue for HY, red for PI, green for HBA and. orange for RA. All distances between pharmacophore features are reported in angstroms

From the above description, we known that the best pharmacophore models for μ, δ and κ agonists contained four, five and five features, respectively. For μ subtype, the best model consisted of four features: two hydrogen-bond acceptor (HBA), one ring aromatic (RA) and one positive ionizable function (PI) (Fig. 1a). For δ subtype, the best model consisted of five features: one HBA, three hydrophobic points (HY) and one PI (Fig. 1b). For κ subtype, the best model consisted of five features: one HBA, two HY, one RA and one PI (Fig. 1c).

In these Hypo1, PI feature was a common characteristic for every subtype. Therefore PI was an essential feature in opioid-agonist interaction. This characteristic could also be found from many experiments and computational models. From these Hypo1, we also found that μ agonists could form two strong hydrogen bonds, while δ and κ ones form only one; and that δ and κ agonists could form many HY, while μ ones could form only one RA. These results showed that HBA feature played an important role in activating analgesia for μ agonists, whereas HY feature played an important role in activating δ and κ subtype interaction.

Comparison with reported models

A summary supported by computer modeling studies was done by Filizola et al. who pointed out the chemical, structural and physicochemical properties of μ, δ and κ opioid agonists [75]. From 12 selected opioid agonists (morphine, hydromorphone, nalbuphine, xorphanol, butorphanol, dezocine, etorphine, fentanyl, lofentanyl, carfentanyl, SIOM and COMP1), the chemical moieties common to three different sets of opioid receptor agonists with significant affinity for each of the three receptor types, μ, δ or κ were identified. Using a distance analysis approach, common geometric arrangements of these chemical moieties were found for selecting μ δ or κ subtype agonists. They may be regarded as the non-specific recognition motifs engaged in the non-specific 3D recognition pharmacophore at μ δ and κ opioid receptors. Analysis of these properties suggested that agonists at δ have the unique requirement of larger volume and agonists at μ have the unique requirement of larger free energy of solvation. It could be said that our pharmacophore models were in accord with these results. Larger volume needed more HY features, and larger free energy of salvation needed more hydrogen binding interaction.

Recently, Singh et al. constructed a 3D pharmacophore model of salvinorin A derivatives using Catalyst software [76]. Their pharmacophore model consisted of two HBA and three HY. That was in agreement with our models except for one positive ionizable group feature. As is known, opioid receptor ligands require protonated nitrogen for high affinity binding. However, salvinorin A is a structurally unique, non-nitrogenous κ opioid receptor agonist; it does not agree with any of the currently accepted pharmacophores of κ opioid receptor ligands, or opioid pharmacophores in general, and demonstrates a new structural class of κ opioid receptor agonists. Therefore, we could say that salvinorins were a very special kind of molecule.

Analysis of opioid receptor-agonist interaction from homology modeling and molecular docking

In above pharmacophore models, we had obtained a general view of chemical features for every opioid subtype

Table 3 Output of the score hypothesis process on the training set by Catalyst/HypoGen

μ opioid agonists					δ opioid agonists					κ opioid agonists				
No.	Activity K_i(nM)[a]	Estimated K_i (nM)	Error[b]	Ref.	No.	Activity K_i (nM)	Estimated K_i (nM)	Error	Ref.	No.	Activity K_i (nM)	Estimated K_i (nM)	Error	Ref.
Cm[c]1	0.05	0.38	+7.7	[21]	Cd[c]1	0.023	0.032	+1.4	[19]	Ck[c]1	0.054	0.029	-1.9	[20]
Cm2	0.09	0.091	+1	[18]	Cd2	0.06	0.86	+14	[21]	Ck2	0.11	0.078	-1.4	[22]
Cm3	0.21	0.57	+2.7	[23]	Cd3	0.11	1.8	+17	[24]	Ck3	0.17	1	+6	[25]
Cm4	0.21	1.5	+7	[26]	Cd4	0.23	1.4	+6.1	[27]	Ck4	0.31	2.7	+8.8	[28]
Cm5	0.37	1.4	+3.8	[29]	Cd5	0.6	0.26	-2.3	[19]	Ck5	0.43	0.92	+2.1	[30]
Cm6	0.6	6.4	+11	[31]	Cd6	0.74	5.6	+7.5	[32]	Ck6	0.45	2	+4.5	[10]
Cm7	0.61	0.57	-1.1	[33]	Cd7	2.9	3.5	+1.2	[32]	Ck7	0.58	0.99	+1.7	[20]
Cm8	0.62	0.47	-1.3	[34]	Cd8	3.2	2.3	-1.4	[19]	Ck8	1.3	2.8	+2.2	[25]
Cm9	2.5	0.99	-2.5	[26]	Cd9	3.5	2.2	-1.6	[27]	Ck9	1.3	0.5	-2.6	[35]
Cm10	23	7.8	-2.9	[36]	Cd10	7	6.6	-1.1	[37]	Ck10	1.5	2.8	+1.9	[22]
Cm11	23	9.3	-2.5	[29]	Cd11	15	51	+3.4	[24]	Ck11	4.9	9.6	+2	[38]
Cm12	38	22	-1.7	[39]	Cd12	35	7.9	-4.4	[40]	Ck12	5.6	53	+9.6	[26]
Cm13	50	33	-1.5	[39]	Cd13	37	6	-6.2	[32]	Ck13	29	9.7	-3	[41]
Cm14	92	220	+2.4	[42]	Cd14	44	16	-2.8	[43]	Ck14	43	1.9	-23	[10]
Cm15	220	370	+1.7	[42]	Cd15	220	34	-6.4	[43]	Ck15	84	130	+1.5	[32]
Cm16	390	190	-2.1	[39]	Cd16	290	880	+3	[40]	Ck16	99	22	-4.4	[32]
Cm17	600	370	-1.6	[42]	Cd17	650	800	+1.2	[39]	Ck17	240	260	+1.1	[26]
Cm18	780	200	-3.9	[44]	Cd18	690	1500	+2.1	[21]	Ck18	550	82	-6.7	[45]
Cm19	1900	170	-12	[21]	Cd19	1400	150	-9.1	[40]	Ck19	620	140	-4.5	[32]
Cm20	2400	1000	-2.3	[46]	Cd20	2500	1100	-2.3	[47]	Ck20	900	470	-1.9	[48]
					Cd21	5800	1800	-3.2	[45]	Ck21	3000	3400	+1.1	[49]
					Cd22	8900	3400	-2.6	[50]					

[a] Activity scale: +++, <10 nM (highly active); ++, 10-500 nM (moderately active); +, >500 nM (inactive)

[b] The error factor is computed as the ratio of the measured activity to the activity estimated by the hypothesis or the inverse if estimated is greater than measured

[c] Cm is the shortcut of the compound of mu subtype, Cd is that of delta and Ck is that of kappa

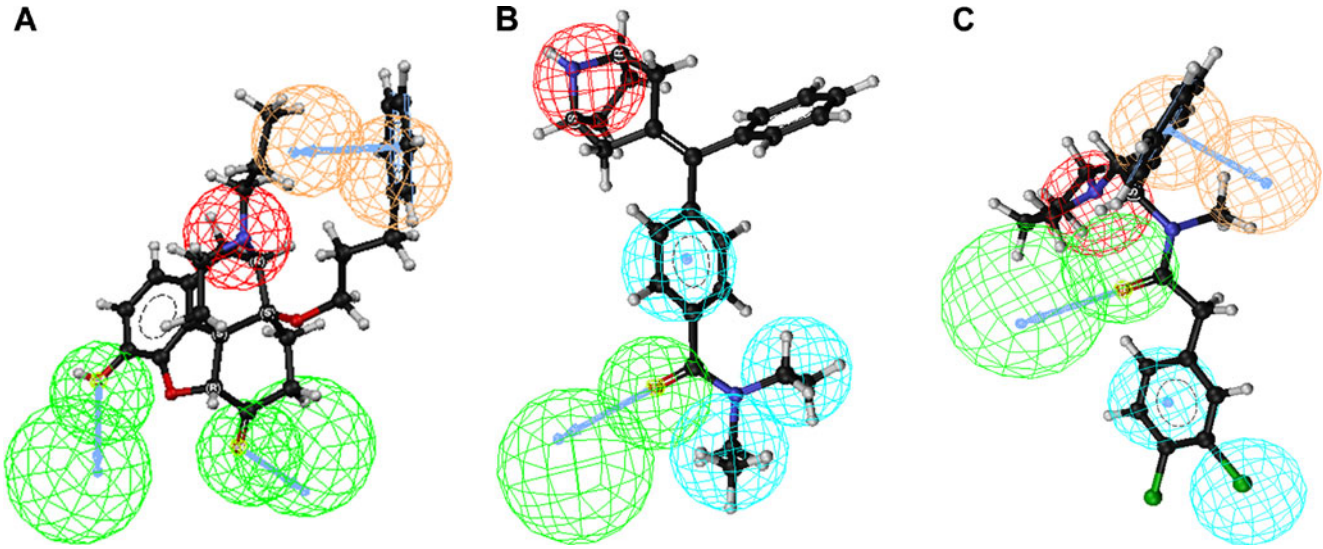

Fig. 2 Pharmacophore mapping of the conformations of these representatives, Cm2, Cd1 and Ck1, was produced by Catalyst4.10 software. (**a**), (**b**) and (**c**) were the pharmacophore mapping complexes of μ δ and κ subtype, separately. Pharmacophore features are color-coded with the same as Fig. 1

agonists. Then, structure-based methods were applied for further understanding specific receptor-agonist interaction. According to these complexes obtained by homology modeling and molecular docking, we could clearly see specific residues interacting with agonists and space-arrangement of all kinds of common chemical features. Therefore, from the large amount of information above, we could be detailed in analysis of receptor-agonist interaction for every subtype.

μ opioid receptor-agonist interaction

From docking complexes, we could see specific residues forming different kinds of interaction, such as hydrogen-bond interaction, ionic interaction and so on.

In the complex of μ subtype and Cm2 (Fig. 5a), there was an ionic interaction between the cationic amino group of Cm2 and carboxylate side chain of Asp149 in TMIII. For μ subtype, the amino acid residue Asp149 in TMIII was predicted to be a key binding site of the cationic amino group in μ selective ligands by mutation studies of opioid receptors [77]. Also, the phenolic hydroxy group of Cm2 could form one hydrogen bond with the phenolic hydroxyl group of Tyr150 at TMIII, which was proposed to be major forces for binding agonists.

At the same time, enol group of Cm2 should form a hydrogen bonding interaction from pharmacophore mapping (Fig. 2a). Although no reasonable hydrogen bond was formed in this complex, enol group of morphine and imidazole group of His299 at TMVI was very close, and thus the third hydrogen bonding interaction was very probably formed between them.

Our results were supported by other experimental results. Chimeric receptors of μ and δ subtypes were expressed systematically and applied for structure-activity relationship SAR) studies to elucidate the ligand binding site of the receptors. As a result, it was proposed that the TMV-VII domains of the μ opioid receptor were involved in recognition and binding of morphine [78]. Previous modeling based on the experiments was in agreement with our study [79].

δ opioid receptor-agonist interaction

From Fig. 5b, two residues, Asp128 and Tyr129 at TMIII, the same as those in μ subtype, were key residues functioning to bind agonists. The carboxyl group of Asp128 at TMIII formed an ionic interaction with the cationic amino group (N-terminal) of Cd1. The side chain of Tyr129 at TMIII formed a hydrogen bond with the carbonyl group of Cd1. Meanwhile, many hydrophobic residues were around those hydrophobic groups in compound Cd1. So many hydrophobic interactions were in δ subtype-agonist complex, and therefore, we could affirm that hydrophobic interaction was greatly attributed to binding agonists.

Besides complete consistency with above pharmacophore mapping, our results were in accord with those of Pogozheva et al. They studied the interaction of BW373U86 binding to δ opioid receptor and found that there was an ionic interaction between the ligand and the side chain carboxyl group of Asp128 at TMIII [80]. Moreover, their interactions consisted of particularly large amounts of hydrophobic interaction.

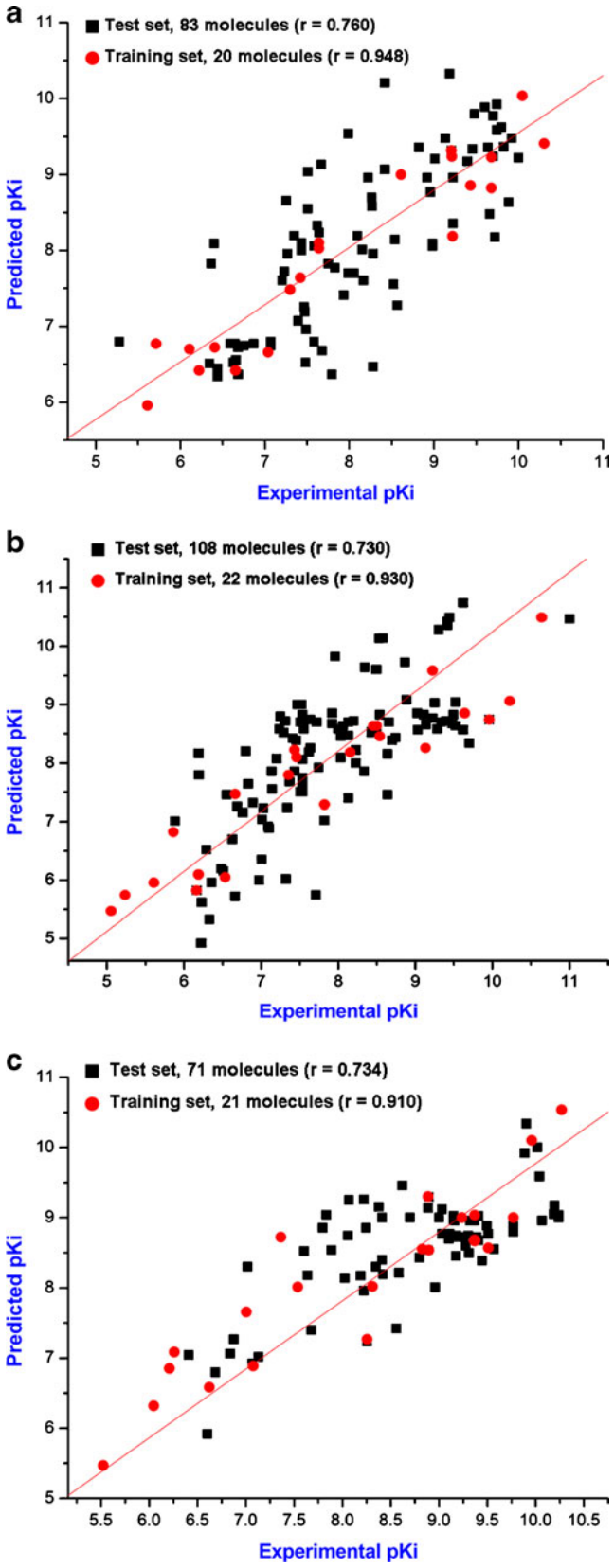

Fig. 3 Graphs showing the correlation between experimental and predicted activities (pK_i = -logK_i) of training set and test set were produced. These sets belong to Hypo1 of every subtype. (**a**), (**b**) and (**c**) were the correlation of μ, δ and κ subtype, separately. Correlation was color-coded with red points for training set compounds, and black boxes for test set compounds. The red line was the correlation curve of training set

κ opioid receptor-agonist interaction

In κ subtype-Ck1 complex (Fig. 5c), like μ and δ subtype, the carboxyl group of Asp138 at TMIII formed an ionic interaction with the cationic amino group (N-terminal) of Ck1. The ionic interaction could be confirmed by previous site-directed mutagenesis studies and molecular dynamics simulation of the receptor-ligand complex [54, 81, 82].

It could also be seen that there was a hydrogen bonding interaction between the side chain of Tyr312 at TMVII and the carbonyl group of Ck1. This hydrogen bond was a specific interaction for κ subtype, which was not found in μ and δ subtype. There were also a few experiments certifying the key residue, Tyr312, in binding agonists [83].

In Fig. 5c, a π-π interaction could be clearly found between aromatic functionality of Tyr139 at TMIII and the phenyl group of Ck1. This interaction was greatly different with that in μ and δ subtype. Whether this π-π interaction was a key factor for selectivity of κ subtype was still needed to be verified.

Analysis from docking complexes together with pharmacophore models

Further modeling was carried on by pharmacophore mapping onto docking complexes (Fig. 6). Their interactive graphs of three subtype-agonist complexes together with common features were clearly shown. Therefore, we could easily analyze their interaction from these new complexes.

Table 4 Sensitivity and specificity of training set for the best models and r_m^2 values of the test set compounds

	SE[a]	SP[b]	r^2	r_m^{2c}
μ opioid agonists	16	0.25	0.577	0.435
δ opioid agonists	0.94	0.83	0.532	0.436
κ opioid agonists	17	0.25	0.539	0.283

[a] SE: sensitivity, which is defined as (true positives)/(true positives + false negatives) for the best models

[b] SP: specificity (SP), which is defined as (true negatives)/(true negatives + false positives)

[c] r_m^2 [65]: a statistic for external validation. The parameters r^2 and r_0^2 are squared correlation coefficient values between observed and predicted response values of the test set compounds with and without intercept respectively

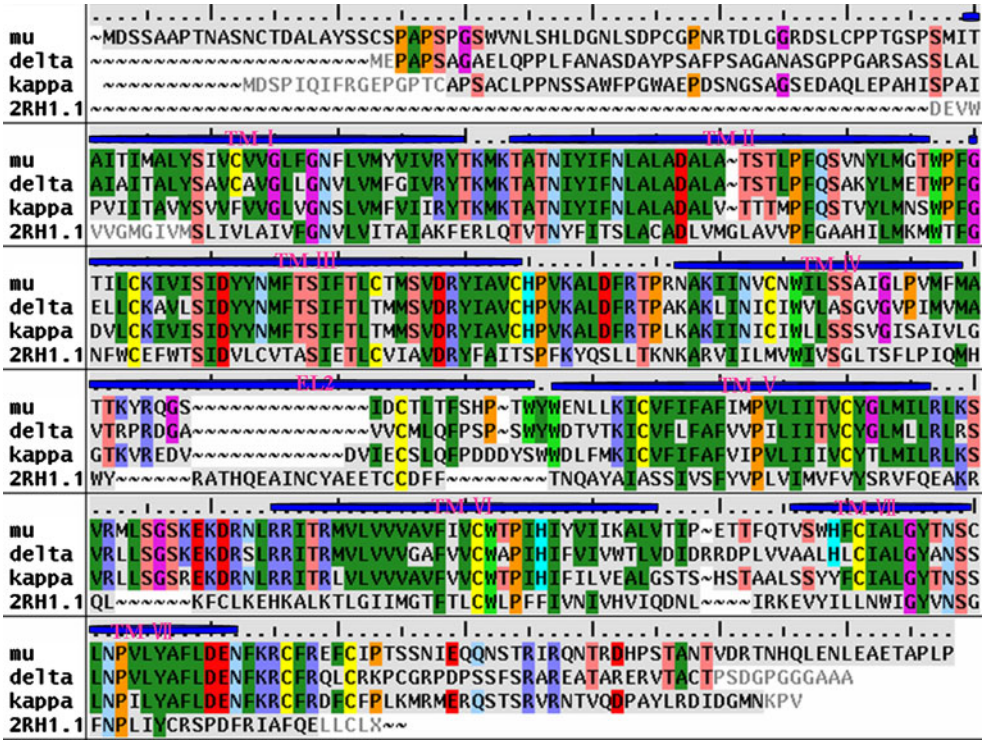

Fig. 4 The alignment of every subtype with β2-AR crystal structure was produced by the Prime module in Schrödinger package. The residues were displayed by Residue Matching mode. Different matching residues were shown by different color

Firstly, above analysis, for example, residue Asp which could form ionic interaction in TMIII and all kinds of hydrogen bonds were clearly seen. Secondly, hydrophobic interaction playing a key role was also easily found, which was difficult both in solo pharmacophore models and docking complexes. For example, in δ subtype, those hydrophobic residues, Phe222, Trp274 and Ile304 were picked out, because they were closer to HY feature than other hydrophobic residues. Same as δ subtype, in κ subtype, a hydrophobic residue, Phe214, was picked out

Implication for selective opioid agonist design

As is well known, designing specific κ opioid receptor agonists is a very interesting topic for developing new

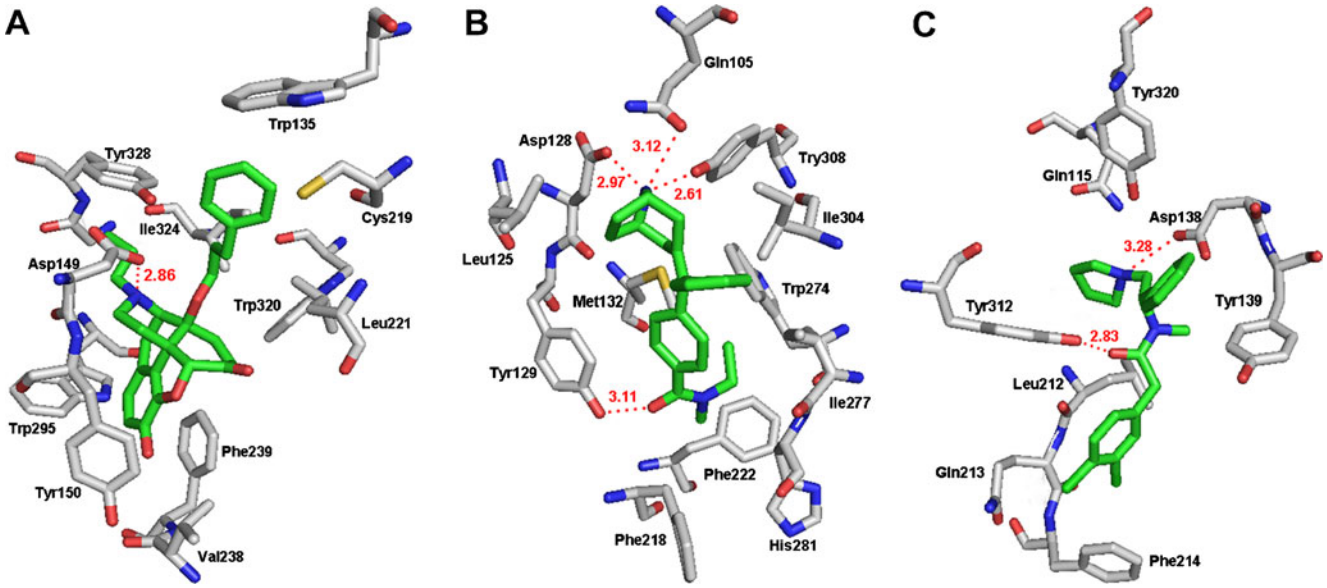

Fig. 5 The docking of the homology models of all subtypes with their representative agonists were produced by Induced Fit Docking program in Schrödinger package. (**a**) (**b**) and (**c**) were docking complexes of μ-Cm2, δ-Cd1 and κ-Ck1, separately

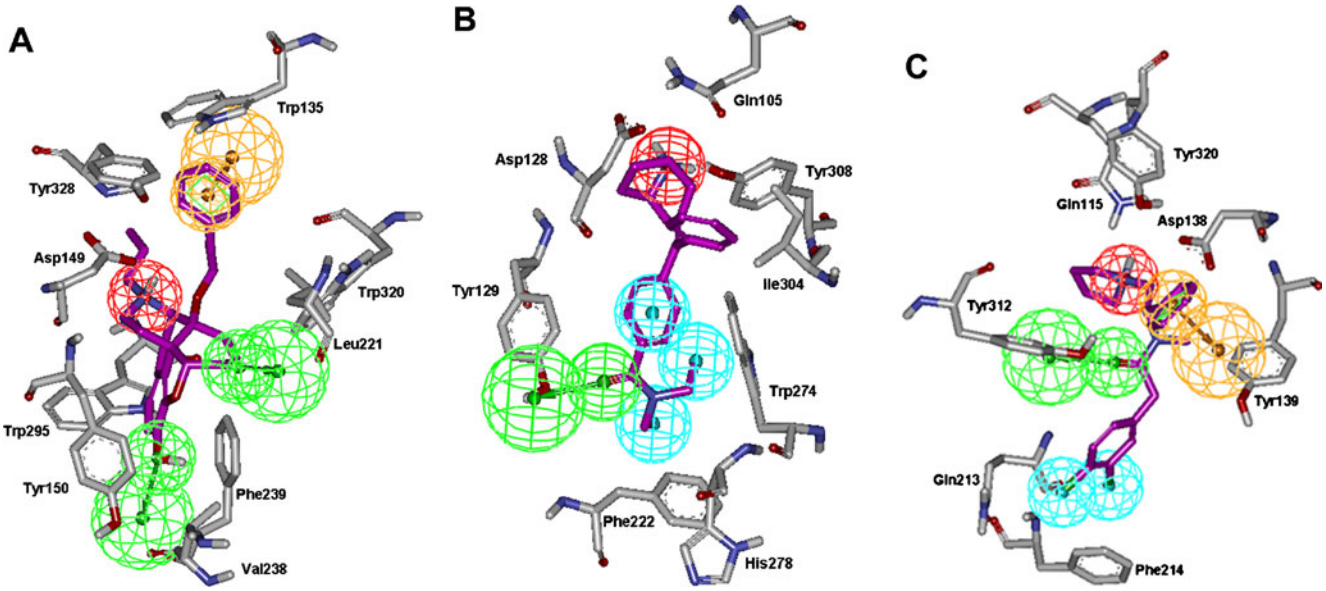

Fig. 6 The best pharmacophore models were superimposed into the active sites of their corresponding docking complexes by the protocol implemented in Discovery Studio 2.1. (**a**), (**b**) and (**c**) were the mapping complexes of pharmacophore models and docking complexes of μ, δ and κ subtype, separately. Pharmacophore features are color-coded the same as Fig. 1

analgesics. From above discussion, we saw that a hydrogen bonding interaction between the side chain of Tyr312 at TMVII and the carbonyl group of Ck1 was formed, whereas there was no strong interaction for μ or δ subtype in that position. Besides, κ agonists could form a π-π interaction with Tyr139 at TMIII, whereas μ and δ ones formed one hydrogen bond separately in that place. Given above different interaction, we should take suitable measures to design new selective κ agonists, such as strengthening the polarity around the carbonyl group of Ck1, besides, eliminating the polarity around the phenyl group of Ck1 or replacing the groups at this position with aromatic rings.

Pharmacophore mapping onto docking complexes should be a practical method to more clearly show receptor-ligand interaction. By this method, hydrophobic interaction which played a key role in binding agonists could also be clearly shown, especially for δ subtype. When we design new δ subtype agonists, we can strengthen the hydrophobic interaction around those residues, Phe222, Trp274 and Ile304, by transforming a few hydrophobic groups.

Conclusions

In the above work, ligand-based and receptor-based drug design methods were implemented together and subtype characteristics of opiod agonists were clearly described.

Three high-quality pharmacophore models of opioid receptor subtype agonists were generated by the Catalyst/HypoGen program. The best pharmacophore models for μ, δ and κ agonists contained four, five and five features, respectively. The pharmacophore mapping conformations were extended. To validate our pharmacophore further, the other available compounds were used as test set. For the best hypothesis of three subtypes, the correlation of μ δ and κ agonists was 0.760, 0.730 and 0.734, separately. Every kind of compounds distributed uniformly. Therefore, these pharmacophore models could be used for virtual screening.

Meanwhile, the three-dimensional structures of three receptor subtypes were modeled based on the crystal structure of β2-adrenergic receptor, and induced-fit docking was conducted further. According to the pharmacophore models and docking results, the similarities and differences among three types of agonists were identified. Almost all the ligands had an ionic interaction with residue Asp in the third transmembrane helix (TMIII). The differences among them were also obvious. μ agonists could form two strong hydrogen bonds, whereas δ and κ ones form many hydrophobic interactions; κ agonists could form strong hydrogen bond with Tyr at TMVII, whereas that interaction was not found in δ and μ ones; δ and μ ones could form one hydrogen bond with the Tyr at TMIII, whereas κ ones form a π-π interaction, which should be crucial for the development of novel selective analgesic drugs.

Acknowledgments This work was supported by National Natural Science Foundation of China (Grants 30600785 and 30973642), the Fundamental Research Funds for the Central Universities (Grant 0914035) and Key 863 High-Tech Program (Grant 2006AA020404).

References

1. Zhang AZ, Pasternak GW (1981) Ontogeny of opioid pharmacology and receptors: high and low affinity site differences. Eur J Pharmacol 73:29–40
2. Pasternak GW (2001) Insights into mu opioid pharmacology the role of mu opioid receptor subtypes. Life Sci 68:2213–2219
3. Martin TJ, Eisenach JC (2001) Pharmacology of opioid and nonopioid analgesics in chronic pain states. J Pharmacol Exp Ther 299:811–817
4. Trescot AM, Datta S, Lee M, Hansen H (2008) Opioid pharmacology. Pain Physician 11:S133–S153
5. Zhu Y, King MA, Schuller AG et al (1999) Retention of supraspinal delta-like analgesia and loss of morphine tolerance in delta opioid receptor knockout mice. Neuron 24:243–252
6. Cahill CM, Morinville A, Hoffert C, O'Donnell D, Beaudet A (2003) Up-regulation and trafficking of delta opioid receptor in a model of chronic inflammation: implications for pain control. Pain 101:199–208
7. Bao L, Jin SX, Zhang C et al (2003) Activation of delta opioid receptors induces receptor insertion and neuropeptide secretion. Neuron 37:121–133
8. DeHaven-Hudkins DL, Dolle RE (2004) Peripherally restricted opioid agonists as novel analgesic agents. Curr Pharm Des 10:743–757
9. Holzgrabe U, Brandt W (2003) Mechanism of action of the diazabicyclononanone-type kappa-agonists. J Med Chem 46:1383–1389
10. Soukara S, Maier CA, Predoiu U, Ehret A, Jackisch R, Wunsch B (2001) Methylated analogues of methyl (R)-4-(3, 4-dichlorophenylacetyl)- 3-(pyrrolidin-1-ylmethyl)piperazine-1-carboxylate (GR-89, 696) as highly potent kappa-receptor agonists: stereoselective synthesis, opioid-receptor affinity, receptor selectivity, and functional studies. J Med Chem 44:2814–2826
11. Johnson H (1978) Quantitative stereo-structure-activity relationships I. Opiate receptor binding. NIDA Res Monogr 146–158
12. Ray SK, Basak SC, Raychaudhury C, Roy AB, Ghosh JJ (1982) A quantitative structure-activity relationship study of N-alkylnorketobemidones and triazinones using structural information content. Arzneimittelforschung 32:322–325
13. Podlogar BL, Poda GI, Demeter DA et al. (2000) Synthesis and evaluation of 4-(N, N-diarylamino)piperidines with high selectivity to the delta-opioid receptor: a combined 3D-QSAR and ligand docking study. Drug Des Discov 17:34–50
14. Huang XQ, Jiang HL, Luo XM et al (2000) Molecular modeling on solvent effect and interaction mechanism of fentanyl analogs to mu-opioid receptor. Acta Pharmacol Sin 21:46–54
15. Peng Y, Keenan SM, Zhang Q, Welsh WJ (2005) 3D-QSAR comparative molecular field analysis on delta opioid receptor agonist SNC80 and its analogs. J Mol Graph Model 24:25–33
16. Wang XH, Tang Y, Xie Q, Qiu ZB (2006) QSAR study of 4-phenylpiperidine derivatives as mu opioid agonists by neural network method. Eur J Med Chem 41:226–232
17. Li W, Tang Y, Xie Q, Sheng W, Qiu ZB (2006) 3D-QSAR studies of orvinol analogs as kappa-opioid agonists. J Mol Model 12:877–884
18. Greiner E, Spetea M, Krassnig R et al. (2003) Synthesis and biological evaluation of 14-alkoxymorphinans. 18. N-substituted 14-phenylpropyloxymorphinan-6-ones with unanticipated agonist properties: extending the scope of common structure-activity relationships. J Med Chem 46:1758–1763
19. Carson JR, Coats SJ, Codd EE et al. (2004) N, N-dialkyl-4-[(8-azabicyclo[3.2.1]-oct-3-ylidene)phenylmethyl]benzamides, potent, selective delta opioid agonists. Bioorg Med Chem Lett 14:2109–2112
20. Kumar V, Marella MA, Cortes-Burgos L et al. (2000) Arylacetamides as peripherally restricted kappa opioid receptor agonists. Bioorg Med Chem Lett 10:2567–2570
21. Breslin HJ, Cai C, Miskowski TA et al. (2006) Identification of potent phenyl imidazoles as opioid receptor agonists. Bioorg Med Chem Lett 16:2505–2508
22. Chu GH, Gu M, Cassel JA et al. (2006) Novel phenylamino acetamide derivatives as potent and selective kappa opioid receptor agonists. Bioorg Med Chem Lett 16:645–648
23. Macdougall JM, Zhang XD, Polgar WE, Khroyan TV, Toll L, Cashman JR (2004) Synthesis and biological evaluation of some 6-arylamidomorphines as analogues of morphine-6-glucuronide. Bioorg Med Chem 12:5983–5990
24. Breslin HJ, Miskowski TA, Rafferty BM et al. (2004) Rationale, design, and synthesis of novel phenyl imidazoles as opioid receptor agonists for gastrointestinal disorders. J Med Chem 47:5009–5020
25. Anzini M, Canullo L, Braile C et al. (2003) Synthesis, biological evaluation, and receptor docking simulations of 2-[(acylamino) ethyl]-1, 4-benzodiazepines as kappa-opioid receptor agonists endowed with antinociceptive and antiamnesic activity. J Med Chem 46:3853–3864
26. Jordan AD, Orsini MJ, Middleton SA et al. (2005) 8-(Heteroaryl) phenalkyl-1-phenyl-1, 3, 8-triazaspiro[4.5]decan-4-ones as opioid receptor modulators. Med Chem 1:601–610
27. Coats SJ, Schulz MJ, Carson JR et al. (2004) Parallel methods for the preparation and SAR exploration of N-ethyl-4-[(8-alkyl-8-azabicyclo[3.2.1]oct-3-ylidene)-aryl-methyl]-benzam ides, powerful mu and delta opioid agonists. Bioorg Med Chem Lett 14:5493–5498
28. Kumar V, Guo D, Cassel JA et al. (2005) Synthesis and evaluation of novel peripherally restricted kappa-opioid receptor agonists. Bioorg Med Chem Lett 15:1091–1095
29. Dardonville C, Fernandez-Fernandez C, Gibbons SL et al. (2006) Synthesis and pharmacological studies of new hybrid derivatives of fentanyl active at the mu-opioid receptor and I2-imidazoline binding sites. Bioorg Med Chem 14:6570–6580
30. Azzolina O, Collina S, Linati L et al. (2001) Enantiomers of 2-[(Acylamino)ethyl]-1, 4-benzodiazepines, potent ligands of kappa-opioid receptor: chiral chromatographic resolution, configurational assignment and biological activity. Chirality 13:606–612
31. Hiebel AC, Lee YS, Bilsky E et al. (2007) Probes for narcotic receptor mediated phenomena. 34. Synthesis and structure-activity relationships of a potent mu-agonist delta-antagonist and an exceedingly potent antinociceptive in the enantiomeric C9-substituted 5-(3-hydroxyphenyl)-N-phenylethylmorphan series. J Med Chem 50:3765–3776
32. Trabanco AA, Aerts N, Alvarez RM et al. (2007) 4-Phenyl-4-[1H-imidazol-2-yl]-piperidine derivatives as non-peptidic selective delta-opioid agonists with potential anxiolytic/antidepressant properties. Part 2. Bioorg Med Chem Lett 17:3860–3863
33. Lattanzi R, Spetea M, Schullner F et al. (2005) Synthesis and biological evaluation of 14-alkoxymorphinans. 22. (1) Influence of the 14-alkoxy group and the substitution in position 5 in 14-alkoxymorphinan-6-ones on in vitro and in vivo activities. J Med Chem 48:3372–3378

34. Schutz J, Spetea M, Koch M et al. (2003) Synthesis and biological evaluation of 14-alkoxymorphinans. 20. 14-phenylpropoxymetopon: an extremely powerful analgesic. J Med Chem 46:4182–4187
35. Chu GH, Gu M, Cassel JA et al. (2005) Potent and highly selective kappa opioid receptor agonists incorporating chroman- and 2, 3-dihydrobenzofuran-based constraints. Bioorg Med Chem Lett 15:5114–5119
36. Dardonville C, Jagerovic N, Callado LF, Meana JJ (2004) Fentanyl derivatives bearing aliphatic alkaneguanidinium moieties: a new series of hybrid molecules with significant binding affinity for mu-opioid receptors and I2-imidazoline binding sites. Bioorg Med Chem Lett 14:491–493
37. Coop A, Rothman RB, Dersch C et al. (1999) delta Opioid affinity and selectivity of 4-hydroxy-3-methoxyindolomorphinan analogues related to naltrindole. J Med Chem 42:1673–1679
38. Beguin C, Richards MR, Wang Y et al. (2005) Synthesis and in vitro pharmacological evaluation of salvinorin A analogues modified at C(2). Bioorg Med Chem Lett 15:2761–2765
39. Page D, Nguyen N, Bernard S et al. (2003) New scaffolds in the development of mu opioid-receptor ligands. Bioorg Med Chem Lett 13:1585–1589
40. Kim IJ, Ullrich T, Janetka JW et al. (2003) Diaryldimethylpiperazine ligands with mu- and delta-opioid receptor affinity: Synthesis of (+)-4-[(alphaR)-alpha-(4-allyl-(2S, 5S)-dimethylpiperazin-1-yl)-(3-hydroxyp henyl)methyl]-N-ethyl-N-phenylbenzamide and (-)-4-[(alphaR)-alpha-(2S, 5S)-dimethylpiperazin-1-yl)-(3-hydroxyphenyl)met hyl]-N-ethyl-N-phenylbenzamide. Bioorg Med Chem 11:4761–4768
41. Chu GH, Gu M, Cassel JA et al. (2007) Novel malonamide derivatives as potent kappa opioid receptor agonists. Bioorg Med Chem Lett 17:1951–1955
42. Loriga G, Manca I, Murineddu G et al. (2006) Synthesis of 3, 6-diazabicyclo[3.1.1]heptanes as novel ligands for the opioid receptors. Bioorg Med Chem 14:676–691
43. Trabanco AA, Pullan S, Alonso JM et al. (2006) 4-Phenyl-4-[1H-imidazol-2-yl]-piperidine derivatives, a novel class of selective delta-opioid agonists. Bioorg Med Chem Lett 16:146–149
44. Pinna GA, Cignarella G, Loriga G et al. (2002) N-3(9)-arylpropenyl-N-9(3)-propionyl-3, 9-diazabicyclo[3.3.1]nonanes as mu-opioid receptor agonists. Effects on mu-affinity of arylalkenyl chain modifications. Bioorg Med Chem 10:1929–1937
45. Grundt P, Williams IA, Lewis JW, Husbands SM (2004) Identification of a new scaffold for opioid receptor antagonism based on the 2-amino-1, 1-dimethyl-7-hydroxytetralin pharmacophore. J Med Chem 47:5069–5075
46. Ho GD, Bercovici A, Tulshian D et al. (2007) Synthesis and structure-activity relationships of 4-hydroxy-4-phenylpiperidines as nociceptin receptor ligands: Part 1. Bioorg Med Chem Lett 17:3023–3027
47. Caldwell JP, Matasi JJ, Zhang H, Fawzi A, Tulshian DB (2007) Synthesis and structure-activity relationships of N-substituted spiropiperidines as nociceptin receptor ligands. Bioorg Med Chem Lett 17:2281–2284
48. Wentland MP, Sun X, Ye Y, Lou R, Bidlack JM (2003) Redefining the structure-activity relationships of 2, 6-methano-3-benzazocines. Part 2: 8-formamidocyclazocine analogues. Bioorg Med Chem Lett 13:1911–1914
49. Wentland MP, Ye Y, Cioffi CL et al. (2003) Syntheses and opioid receptor binding affinities of 8-amino-2, 6-methano-3-benzazocines. J Med Chem 46:838–849
50. Ho GD, Bercovici A, Tulshian D et al. (2007) Synthesis and structure-activity relationships of 4-hydroxy-4-phenylpiperidines as nociceptin receptor ligands: Part 2. Bioorg Med Chem Lett 17:3028–3033
51. Palczewski K, Kumasaka T, Hori T et al. (2000) Crystal structure of rhodopsin: A G protein-coupled receptor. Science 289:739–745
52. Bourne HR, Meng EC (2000) Structure. Rhodopsin sees the light. Science 289:733–734
53. Luecke H, Schobert B, Lanyi JK, Spudich EN, Spudich JL (2001) Crystal structure of sensory rhodopsin II at 2.4 angstroms: insights into color tuning and transducer interaction. Science 293:1499–1503
54. Iadanza M, Holtje M, Ronsisvalle G, Holtje HD (2002) Kappa-opioid receptor model in a phospholipid bilayer: molecular dynamics simulation. J Med Chem 45:4838–4846
55. Fowler CB, Pogozheva ID, LeVine H 3rd, Mosberg HI (2004) Refinement of a homology model of the mu-opioid receptor using distance constraints from intrinsic and engineered zinc-binding sites. Biochemistry 43:8700–8710
56. Aburi M, Smith PE (2004) Modeling and simulation of the human delta opioid receptor. Protein Sci 13:1997–2008
57. Zhang Y, Sham YY, Rajamani R, Gao J, Portoghese PS (2005) Homology modeling and molecular dynamics simulations of the mu opioid receptor in a membrane-aqueous system. Chembiochem 6:853–859
58. Li W, Tang Y, Zheng YL, Qiu ZB (2006) Molecular modeling and 3D-QSAR studies of indolomorphinan derivatives as kappa opioid antagonists. Bioorg Med Chem 14:601–610
59. Cherezov V, Rosenbaum DM, Hanson MA et al (2007) High-resolution crystal structure of an engineered human beta2-adrenergic G protein-coupled receptor. Science 318:1258–1265
60. Rosenbaum DM, Cherezov V, Hanson MA et al (2007) GPCR engineering yields high-resolution structural insights into beta2-adrenergic receptor function. Science 318:1266–1273
61. Greene J, Kahn S, Savoj H, Sprague P, Teig S (1994) Chemical function queries for 3D database search. J Chem Inf Comput Sci 16:1297–1308
62. Brooks BR, Broccoleri RE, Olafson BD, States DJ, Swaminathan S, Karplus M (1983) CHARMM: a program for macromolecular energy. J Comput Chem 4:187–217
63. Rollinger JM, Haupt S, Stuppner H, Langer T (2004) Combining ethnopharmacology and virtual screening for lead structure discovery: COX-inhibitors as application example. J Chem Inf Comput Sci 44:480–488
64. CATALYST, 4.10. Accelrys Inc. http://www.accelrys.com: San Diego, CA
65. Roy PP, Roy K (2008) On some aspects of variable selection for partial least squares regression models. QSAR Comb Sci 27:302–313
66. Sali A, Blundell TL (1993) Comparative protein modelling by satisfaction of spatial restraints. J Mol Biol 234:779–815
67. Sali A, Overington JP (1994) Derivation of rules for comparative protein modeling from a database of protein structure alignments. Protein Sci 3:1582–1596
68. Chang G, Still WC, Guida WC (1989) An internal coordinate Monte Carlo method for searching conformational space. J Am Chem Soc 111:4379–4386
69. Mohamadi F, Richards NGJ, Guida WC et al (1990) Macromodels-An integrated software system for modeling organic and bioorganic molecules using molecular mechanics. J Comput Chem 11:440–467
70. Glide, 5.0, 2008. Schrödinger, LLC
71. Prime, 2.0, 2008. Schrödinger, LLC
72. Zhang J, Yu K, Zhu W, Jiang H (2006) Neuraminidase pharmacophore model derived from diverse classes of inhibitors. Bioorg Med Chem Lett 16:3009–3014
73. Codd EE, Shank RP, Schupsky JJ, Raffa RB (1995) Serotonin and norepinephrine uptake inhibiting activity of centrally acting analgesics: structural determinants and role in antinociception. J Pharmacol Exp Ther 274:1263–1270

74. DeHaven-Hudkins DL, Burgos LC, Cassel JA et al. (1999) Loperamide (ADL 2-1294), an opioid antihyperalgesic agent with peripheral selectivity. J Pharmacol Exp Ther 289:494–502
75. Filizola M, Villar HO, Loew GH (2001) Differentiation of delta, mu, and kappa opioid receptor agonists based on pharmacophore development and computed physicochemical properties. J Comput Aided Mol Des 15:297–307
76. Singh N, Cheve G, Ferguson DM, McCurdy CR (2006) A combined ligand-based and target-based drug design approach for G-protein coupled receptors: application to salvinorin A, a selective kappa opioid receptor agonist. J Comput Aided Mol Des 20:471–493
77. Surratt CK, Johnson PS, Moriwaki A et al. (1994) mu opiate receptor. Charged transmembrane domain amino acids are critical for agonist recognition and intrinsic activity. J Biol Chem 269:20548–20553
78. Fukuda K, Kato S, Mori K (1995) Location of regions of the opioid receptor involved in selective agonist binding. J Biol Chem 270:6702–6709
79. Sagara T, Egashira H, Okamura M, Fujii I, Shimohigashi Y, Kanematsu K (1996) Ligand recognition in mu opioid receptor: experimentally based modeling of mu opioid receptor binding sites and their testing by ligand docking. Bioorg Med Chem 4:2151–2166
80. Pogozheva ID, Lomize AL, Mosberg HI (1998) Opioid receptor three-dimensional structures from distance geometry calculations with hydrogen bonding constraints. Biophys J 75:612–634
81. Subramanian G, Paterlini MG, Larson DL, Portoghese PS, Ferguson DM (1998) Conformational analysis and automated receptor docking of selective arylacetamide-based kappa-opioid agonists. J Med Chem 41:4777–4789
82. Lavecchia A, Greco G, Novellino E, Vittorio F, Ronsisvalle G (2000) Modeling of kappa-opioid receptor/agonists interactions using pharmacophore-based and docking simulations. J Med Chem 43:2124–2134
83. Thirstrup K, Hjorth SA, Schwartz TW (1996) In Investigation of the Binding Pocket in the Kappa Opioid Receptor by a Combination of Alanine Substitutions and Steric Hindrance Mutagenesis. 27th Meeting of the International Narcotics Research Conference, Poster M30